ACI MATERIALS JOURNAL TECHNICAL PAPER

Title no. 98-M52

Tensile Strain-Hardening Behavior of Polyvinyl Alcohol Engineered Cementitious Composite (PVA-ECC)

by Victor C. Li, Shuxin Wang, and Cynthia Wu

A high-performance polyvinyl alcohol fiber-reinforced engineered cementitious composite (PVA-ECC) for structural applications has been developed under the performance-driven design approach. Fiber, matrix, and fiber/matrix interfacial properties were tailored based on micromechanics models to satisfy the pseudo strain-hardening condition. In this paper, the effects of fiber surface treatment and sand content on the composite performance were experimentally investigated. Results from uniaxial tensile tests show an ultimate strain exceeding 4%, as well as an ultimate strength of 4.5 MPa for the composites, with a moderate fiber volume fraction of 2.0%. The specimens reveal saturated multiple cracking with crack width at ultimate strain limited to below 100 μm. The underlying reason of the distinctly different tensile behavior between normal fiber-reinforced concrete and PVA-ECC is highlighted by the comparison of complementary energy from their fiber bridging stress and crack opening curves.

Keywords: cementitious; crack; strain.

INTRODUCTION

In the past decade, high-performance fiber-reinforced cementitious composites (HPFRCCs) have evolved with intensified research. This advance is due to developments in fiber, matrix, and processing technology, as well as better understanding of the fundamental micromechanics governing composite behavior, particularly, the interaction among fiber, matrix, and interface properties.[1-4] Although it is difficult to give an exact definition, HPFRCCs usually refer to those with macroscopic pseudo strain-hardening behavior in tension.[5] The multiple cracking accompanying pseudo strain-hardening implies high ductility, large energy absorption capacity, and high toughness, which distinguishes HPFRCC from conventional fiber-reinforced concrete (FRC). For FRC, localization of damage occurs immediately after first cracking, leading to tension-softening, with a continuously increasing crack opening.

HPFRCCs are usually achieved by introducing large volume fraction of fibers (typically above 5%). Examples include SIFCON and SIMCON.[6,7] Composites with high fiber volume fractions necessitate special processing such as the slurry-infiltrated technique, and also incur high material cost. In another approach, engineered cementitious composites (ECCs) have been developed[8] that adopt short fibers at typically moderate volume fraction (1 to 2%) and can be produced in either a regular casting process or an extrusion process.[9] For an ECC reinforced with 1.5% by volume high-modulus polyethylene fibers (PE-ECC), a tensile strength exceeding 5.5 MPa, and a tensile strain capacity between 4 and 6% has been achieved, as shown in Fig. 1. After first cracking, the strain-hardening behavior leads to tremendous improvement in ductility and toughness.

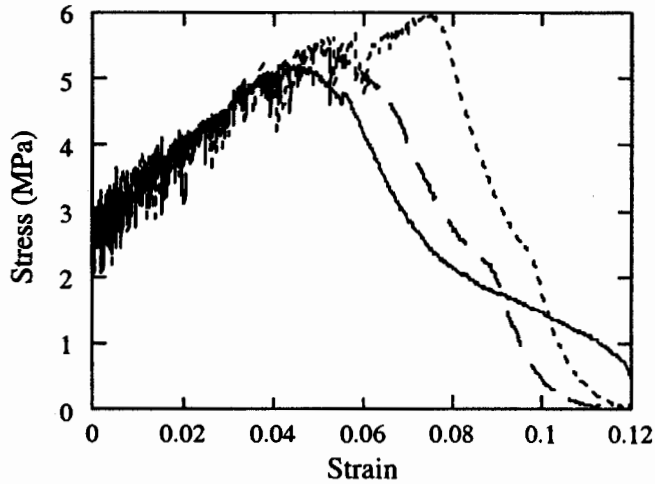

Fig. 1—Typical tensile stress-versus-strain curves of PE-ECC.

Although FRC has been accepted by the practice community since the 1980s, most of its applications are limited to nonstructural use, which can be at least partially attributed to the limited performance, economic constraint, lack of design guidelines, and inconvenient processing. Meanwhile, in constructed facilities, the need for improvement in structural ductility and durability has received increasing attention. Designed for structural applications, ECCs bring extraordinarily high performance as an advanced construction material. Significant contributions to structural ductility, deformation capacity, strength, damage tolerance, and repairability have been demonstrated.[10-12] Specifically, in steel-reinforced ECC (R/ECC), due to the strain-hardening behavior and large strain capacity, ECC can carry load well above the yield point of steel reinforcement.[13] The high shear capacity of ECC helps to reduce or even eliminate the need for shear reinforcements.[14-16] Small crack width limited to below 0.2 mm delivers superior durability,[17] and the high ductility and compatible deformation of ECC with steel reinforcements lead to high structural damage tolerance and deformability.[18]

Because of its moderate fiber content, ECC can be applied in on-site construction as well as in off-site precast elements. Special versions of ECC with self-compacting rheological behavior have been developed.[19] Extrusion of ECC pipes has been demonstrated.[9] Broad application of PE-ECC,

ACI Materials Journal, V. 98, No. 6, November-December 2001.
MS No. 00-018 was received January 26, 2001, and reviewed under Institute publication policies. Pertinent discussion will be published in the September-October 2002 *ACI Materials Journal* if received by June 1, 2002.

ACI member **Victor C. Li** *is a professor of civil and environmental engineering at the University of Michigan, Ann Arbor, Mich. His research interests include micromechanics-based composite materials design and engineering, and innovative structure design based on advanced materials technology and infrastructure engineering.*

ACI member **Shuxin Wang** *is a graduate student research assistant in the Department of Civil and Environmental Engineering at the University of Michigan. He received his BS and MS from Tsinghua University, Beijing, China. His research interests include the development of engineered cementitious composites and the application of fiber-reinforced plastic reinforcement.*

Cynthia Wu *received her PhD in 2001 from the Department of Civil and Environmental Engineering at the University of Michigan. Her research interests include tailoring of fibers and fiber/matrix interface for ductile composite design.*

however, is hindered by the relative high cost of the PE fiber. Polyvinyl alcohol (PVA) fiber, which typically has a tensile strength between 1600 and 2500 MPa, is considered a promising alternative. The cost of PVA fiber is about 1/8 that of high-modulus PE fiber, and is even lower than that of steel fiber on an equal volume basis. With certain adjustments in fiber and fiber surface properties, PVA fiber offers promise as an ECC reinforcement.

Several research projects have been conducted to develop high-performance cementitious composites with PVA fibers.[20-23] All these composites, however, exhibit quasi-brittle tensile behavior or show very low strain capacities, typically less than 0.5%. They are not classified as high-performance based on the aforementioned criteria. To understand the underlying reasons behind the limited composite performance, the nature of interaction between PVA fibers and the cementitious matrix must be examined. As a hydrophilic fiber, PVA has a strong affinity to hydroxy groups present in the neighboring hydrated cement,[24] which creates a strong chemical bond between fiber and surrounding matrix. In addition, the filament microstructure and low lateral resistance of PVA fibers further promote rupture of a bridging fiber rather than pullout during the opening of a matrix crack. Despite these obstacles, PVA fiber still holds great potential since the interfacial characteristics could be modified. Moreover, the manufacturing process of PVA fiber allows tailoring of fiber geometric and mechanical properties within certain ranges. To translate these potentials of PVA fibers into favorable composite performance, a design approach must be adopted to guide the optimization of the composite behaviors.

In the past decade, a design philosophy has emerged that gives credence to the links that exist between structural performance, composite behavior, and material microstructure. This philosophy, illustrated by the performance-driven design approach (PDDA) (Fig. 2), emphasizes micromechanics as the unifying link between mechanical properties and material microstructures.[25] In this approach, the imposed requirements of structural performance, such as load and deformation capacity, ductility, and durability, are translated into mechanical properties at the material level in terms of strength, ultimate strain, toughness, maximum crack width, and other property specifications. Micromechanics models that relate the material properties to material microstructures serve as powerful analytic tools, providing guidance to constituent material tailoring. It elevates material design from trial-and-error empirical combination of material constituents to systematic engineered selection. In the context of PVA-ECC development, these material constituents are characterized by the fiber, matrix, and interface properties that are discussed at length in the following section. Once a preliminary selection of material constituents has been obtained, they are realized by appropriate processing methods that involve fiber geometry modification and surface treatment, cementitious matrix ingredient design, composite mixture rheological control, mixing and casting method optimization, and curing condition selection. Since some of the processing methods impact several material parameters, some amount of iteration and optimization is inevitable.

This paper focuses on the experimental characterization of tensile behaviors of the PVA-ECC developed under the approach outlined previously. First, the framework of PVA-ECC design is briefly reviewed. The material design and test program are then described. Experimental test results in terms of stress-strain curves and cracking patterns are reported. In the discussion section, comparison between quasibrittle PVA-FRC and PVA-ECC will be made in light of the micromechanics design guidelines for ECC.

RESEARCH SIGNIFICANCE

The brittleness of cementitious materials has been identified as a bottleneck that hinders structural performances such as ductility in shear and tension, and durability. Whereas conventional FRC with tension-softening behavior partially alleviates this bottleneck, strain-hardening cementitious composites have demonstrated significant advantages in structural behavior not achievable by normal FRC. In the present research, an ECC was successfully developed with a tailored PVA fiber. Specifically, ECC containing 2 vol % of a PVA-REC fiber with surface oil coating was demonstrated to have tensile strain capacity in excess of 4%. The results of this research illustrate the significance of micromechanics-based composite design for desirable performance. While PVA-ECC attains high performance, it remains economically feasible for practical engineering use because of its relatively low fiber content. For the same reason, an essentially standard mixing process for normal concrete can be applied to ECC, leading to a potentially broad range of applications in civil infrastructures.

PVA-ECC design framework

The tailoring of the microstructure of the composite is based on the understanding of the mechanical interactions among the fiber, matrix, and interface phases. Under the PDDA, this interaction is quantified by the micromechanics models that provide the link between the composite performance and the micromechanical parameters. Three sets of parameters are involved in the design of PVA-ECC corresponding to the fiber, matrix, and interface phases. The fiber is characterized in terms of volume fraction V_f, fiber length l_f, diameter d_f, elastic modulus E_f, and tensile strength σ_{fu}. The matrix is characterized in terms of its fracture toughness K_m, elastic modulus E_m, and initial flaw size distribution a_0. The fiber and matrix interaction, or interface characteristics, are described by the interfacial frictional stress τ_o, chemical bond G_d, and snubbing coefficient f.[26] The strength reduction factor f' is needed to account for the reduction of fiber strength when pulled at an inclined angle.[27] In addition, another parameter β is introduced to characterize the slip-hardening behavior during fiber pullout, recognizing the hydrophilic nature and microstructure feature of the PVA fiber.[28] Since the low tensile strain capacity of most cementitious materials is identified as the bottleneck property to achieving superior structural performance, the dominant micromechanical model

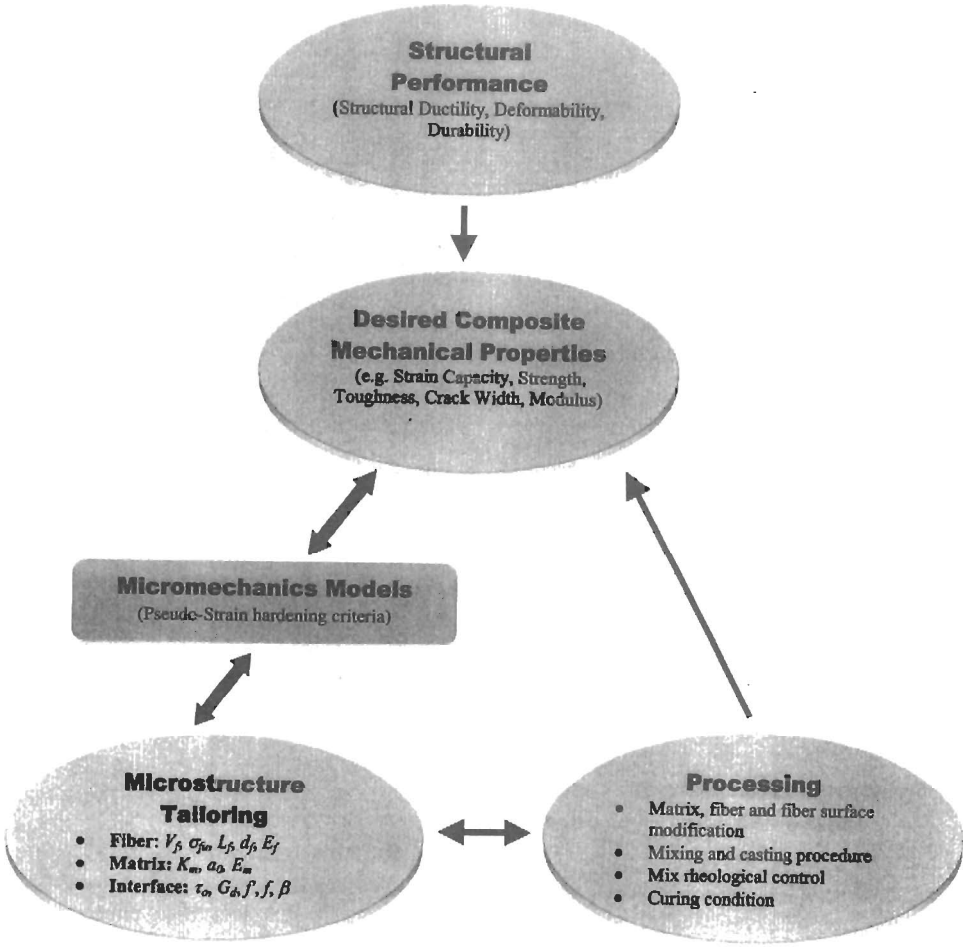

Fig. 2—Performance-driven design approach on PVA-ECC design.

utilized herein is mainly focused on achieving pseudo strain-hardening in tension.

A fundamental requirement for pseudo strain-hardening is that steady state cracking occurs, which requires the crack tip toughness J_{tip} to be less than the complementary energy J_b' calculated from the bridging stress σ versus crack opening δ curve, as illustrated in Fig. 3[25,29]

$$J_{tip} \leq \sigma_0 \delta_0 - \int_0^{\delta_0} \sigma(\delta) d\delta \equiv J_b' \tag{1}$$

$$J_{tip} = \frac{K_m^2}{E_c} \tag{2}$$

where σ_0 is the maximum bridging stress corresponding to the opening δ_0, and E_c is the composite elastic modulus. Equation (1) is obtained by considering the balance of energy changes during extension of the steady-state flat crack. The stress-crack opening relationship $\sigma(\delta)$, which is viewed as a constitutive law of fiber reinforced composites, is derived by utilizing analytic tools of fracture mechanics, micromechanics, and statistics. Specifically, the energetics of tunnel crack propagation along fiber/matrix is used to quantify the debonding process and the bridging force of a fiber with a given embedment length;[30] statistics are introduced to

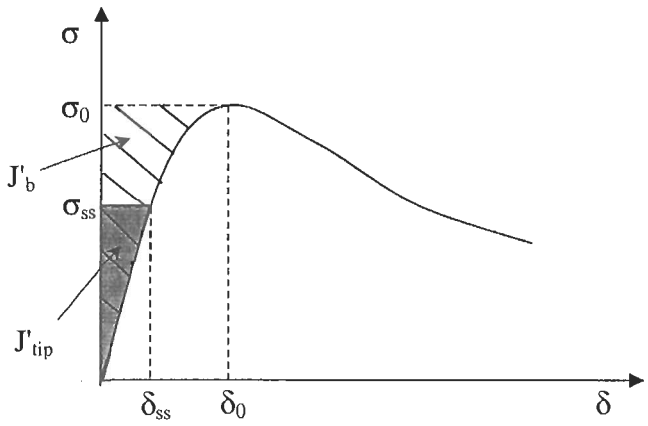

Fig. 3—Typical $\sigma(\delta)$ curve for strain-hardening composite. Hatched area represents complementary energy J_b'. Shaded area represents the crack tip toughness J_{tip}.

describe the random nature of preexisting flaws and the random location and orientation of fibers.[31,32] The random orientation of fibers also necessitates the accounting for the mechanics of interaction between an inclined fiber and the matrix crack. Another condition for pseudo strain-hardening is that the tensile first crack strength σ_{fc} must not exceed the maximum bridging stress σ_0

$$\sigma_{fc} < \sigma_0 \tag{3}$$

Table 1—Properties of Kuraray PVA fibers

Fiber type	Nominal strength, MPa	Fiber diameter, μm	Fiber length, mm	Young's modulus, GPa	Elongation, %
REC	1620	39	12	42.8	6.0
RMU	1660	14	6	60	6.0

Table 2—Mixture proportions by weight

Mixture no.	Oiling agent content, %	V_f, volume %	Cement	Water	Sand	MC*	SP†
1	0.3	2.0	1.0	0.45	0.5	0.0020	None
2	0.3	2.0	1.0	0.45	0.6	0.0020	0.02
3	0.3	2.0	1.0	0.45	0.8	0.0015	0.03
4	0.3	2.0	1.0	0.45	1.0	0.0015	0.03
5	0.5	2.0	1.0	0.45	0.6	0.0015	0.02
6	0.5	2.0	1.0	0.45	0.8	0.0015	0.03
7	0.5	2.0	1.0	0.45	1.0	0.0015	0.03
8	0.5	2.0	1.0	0.45	1.2	0.0015	0.03
9	0.8	2.0	1.0	0.45	0.6	0.0015	0.02
10	0.8	2.0	1.0	0.45	1.0	0.0015	0.03
11	0.8	2.0	1.0	0.45	1.2	0.0015	0.03
12	0.8	2.5	1.0	0.45	1.2	0.0015	0.03
PVA-FRC RMU fiber		2.0	1.0	0.45	0.6	0.0015	0.03

*Hydroxypropyl methylcellulose to cement ratio.
†High-range water-reducing admixture.

where σ_{fc} is determined by the maximum preexisting flaw size max$[a_0]$ and the matrix fracture toughness K_m. Details of these micromechanics analyses can be found in Li and Leung[3] and Li and Wu.[4] Satisfaction of Eq. (1) and (3) is necessary to achieve ECC behavior, otherwise, normal tensile-softening FRC behavior results.

Numerical studies carried out based on the aforementioned micromechanics models produce a set of targeted material microstructure parameters to achieve pseudo strain-hardening behavior.[33] For example, the fiber strength needs to exceed 1000 MPa with minimum fiber elongation of 5% while the preferred fiber diameter is 30 to 50 μm. Constrained by providing effective load transfer and composite processing limit, the fiber length is set to 12 mm in this study. Since the pre-existing flaw size has a certain distribution range, a sufficient margin between complementary energy J_b' and crack tip toughness J_{tip} is desired for developing saturated multiple cracking. This can be achieved by either reducing J_{tip}, which is correlated to matrix toughness as shown in Eq. (2), or increasing J_b'. The latter is more desirable because low matrix toughness implies low first crack strength. Given a reasonable matrix fracture toughness of 0.20 to 0.33 MPa$\sqrt{m}$, maintaining a sufficient margin between J_b' and J_{tip} requires a chemical bond G_d below 2 J/m^2 and an interfacial frictional stress τ_0 between 1.0 and 1.7 MPa, which could be achieved by fiber surface coating. Close cooperation with the PVA fiber manufacturer made these modifications on fiber properties possible. More details on fiber and interface tailoring can be found in Wu.[33]

EXPERIMENTAL PROGRAM

The experimental program serves two purposes, namely verifying the model and searching for an optimal and practical mixture proportioning of PVA-ECC, because some subtle interactions between material constituents still need to be further described by more advanced models. With the guideline provided by the current micromechanics models, however, the search space for an optimal solution has been significantly narrowed.

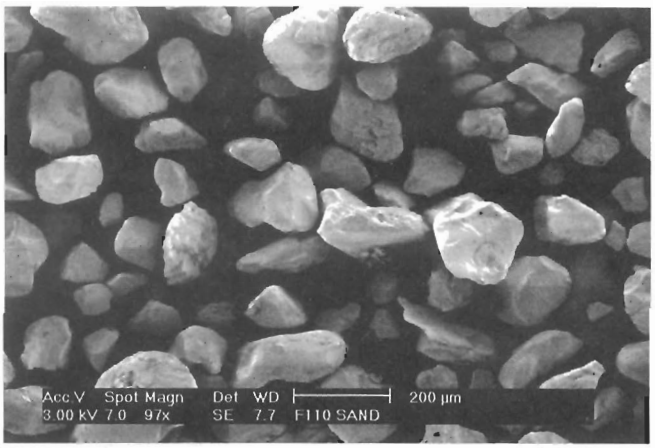

Fig. 4—SEM picture of F110 sand.

A PVA fiber trade-named REC and tailored based on the framework outlined in the previous section was adopted in this study. The fiber properties are listed in Table 1. Two variables were studied in this experimental program. One is the difference in fiber surface treatment, in terms of the content of the oiling coating agent. Higher oiling agent content corresponds to lower chemical bond G_d, and lower interfacial frictional stress τ_0, which can be measured by single fiber pullout test.[27] Three different oiling agent contents, namely, 0.3, 0.5, and 0.8 (% by weight), are investigated in this study. The proprietary oiling agent is coated onto the fiber as a surface treatment in the fiber manufacturing process. Another variable studied is the sand content, which is related to the matrix toughness, as well as the interface properties. Fine sand with a mean size of 110 μm was adopted to maintain low matrix toughness. As shown in Fig. 4, this sand particle has a near-round shape and smooth surface. Fiber volume fraction is set to 2.0 and 2.5%, limited by economic constraint and fresh mixture workability consideration. Water-cement ratio (w/c) is fixed at 0.45 throughout the test. The mixture proportions are tabulated in Table 2.

The mixture was prepared in a small mixer and then cast into plexiglass molds, with moderate vibration. Specimens were demolded after 24 h, then cured in water at room temperature for 28 days. After removal from the curing tank, the specimens were dried in air for 24 h.

A uniaxial tensile test was carried out to characterize the tensile behavior of PVA-ECC. Since some quasibrittle FRCs show apparent strain-hardening behavior under flexural loading, a direct uniaxial tensile test is considered the most convincing way to confirm the strain-hardening behavior of the composite. The coupon specimen used herein measured 304.8 x 76.2 x 12.7 mm. Aluminum plates were glued at the ends of the coupon specimen to facilitate gripping. Tests were conducted in an MTS machine with a 25 kN capacity under displacement control. The loading rate was 0.0025 mm/s throughout the test. Two external linear variable displacement transducers (LVDTs) were attached to specimen surface with a gage length approximately 180 mm to measure the displacement. Further test configuration details can be

Table 3—PVA-ECC tensile test results

Mixture no.	Oiling agent content, %	V_f, %	s/c	First crack strength σ_{fc}, MPa	Ultimate strength σ_{cu}, MPa	Ultimate strain ε_{cu}, %	Crack spacing, mm	Residual crack opening, mm
1	0.3	2.0	0.5	3.45 ± 0.25	4.56 ± 0.70	2.01 ± 0.95	4.9 ± 1.4	42 ± 15
2	0.3	2.0	0.6	3.18 ± 0.12	4.54 ± 0.25	2.43 ± 1.31	6.0 ± 2.9	49 ± 12
3	0.3	2.0	0.8	3.56 ± 0.41	4.45 ± 0.40	1.37 ± 0.44	11.5 ± 2.4	39 ± 16
4	0.3	2.0	1.0	3.97 ± 0.28	4.60 ± 0.23	1.59 ± 0.35	7.5 ± 2.8	44 ± 07
5	0.5	2.0	0.6	2.62 ± 0.27	3.69 ± 0.68	3.71 ± 1.16	3.9 ± 1.4	54 ± 04
6	0.5	2.0	0.8	2.56 ± 0.19	3.98 ± 0.30	4.18 ± 0.52	2.6 ± 0.3	67 ± 09
7	0.5	2.0	1.0	2.66 ± 0.11	4.02 ± 0.40	3.62 ± 0.56	3.5 ± 2.0	52 ± 10
8	0.5	2.0	1.2	3.45 ± 0.14	3.92 ± 0.15	1.64 ± 0.60	6.4 ± 1.0	45 ± 19
9	0.8	2.0	0.6	2.96 ± 0.13	3.92 ± 0.25	1.73 ± 0.29	6.2 ± 0.8	46 ± 17
10	0.8	2.0	1.0	3.11 ± 0.14	4.58 ± 0.38	3.68 ± 1.16	2.5 ± 0.3	71 ± 09
11	0.8	2.0	1.2	2.63 ± 0.32	4.28 ± 0.17	2.48 ± 1.04	3.9 ± 2.4	50 ± 09
12	0.8	2.5	1.2	3.39 ± 0.09	5.00 ± 0.52	4.59 ± 0.36	1.8 ± 0.3	58 ± 10

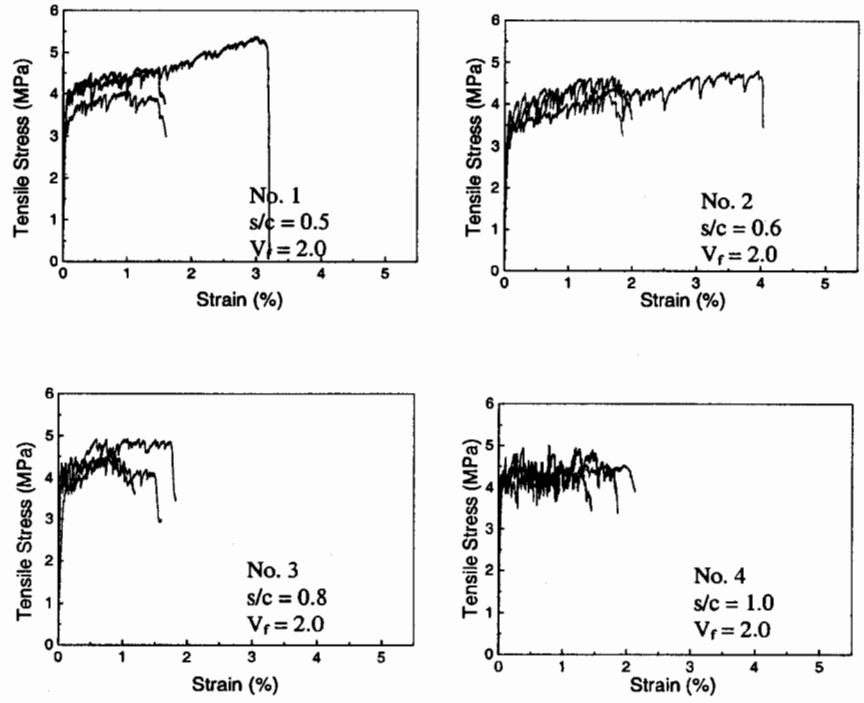

Fig. 5—Tensile stress versus strain curves of PVA-ECC (fiber with 0.3% oiling).

found in the literature.[34] At least three specimens were tested in each case.

During loading, one or two typical cracks were continuously monitored by a calibrated videomicroscope at 200× magnification. After unloading, the specimens were inspected under a magnifier at 50× magnitude, and the average crack spacing was calculated by the gage length divided by the number of visible cracks.

TEST RESULTS

The results of the uniaxial tensile tests in terms of first crack strength, ultimate strength, ultimate strain, crack width, and crack spacing are displayed in Table 3, and the stress-strain curves are presented in Fig. 5 through 7. All specimens show clear pseudo strain-hardening behavior with strain capacities ranging from 1.5 to nearly 5.5%. The first crack strength varies from 2.6 to 3.9 MPa, which is close to the low end of the tensile strength of normal- and high-strength concrete. After first cracking, the load continues to rise without fracture localization. Sequentially developed subparallel cracks contribute to the inelastic strain at increasing stress. In contrast, a single crack that continuously opens while stress decreases is often observed in PVA-FRC. After the peak stress is reached, a localized crack opening occurs at one of the weak sections, which leads to the failure of the composite.

An overview of the stress-strain curves indicates that PVA-ECC with 0.5 and 0.8% oiled fibers have better overall composite performances than those with 0.3% oiled fiber. For the composites with 0.3% oiled fiber, most specimens show a moderate ultimate strain of 2%, except for two that show exceptionally high ultimate strains of 3.1 and 4.0%, achieved with 0.5 and 0.6 sand-cement ratio by weight (*s/c*), respectively. Although these specimens demonstrate the potential for high ductility for the composites with 0.3% oiled fiber, the large variation in ultimate strain indicates a relatively low margin for satisfying the strain-hardening condi-

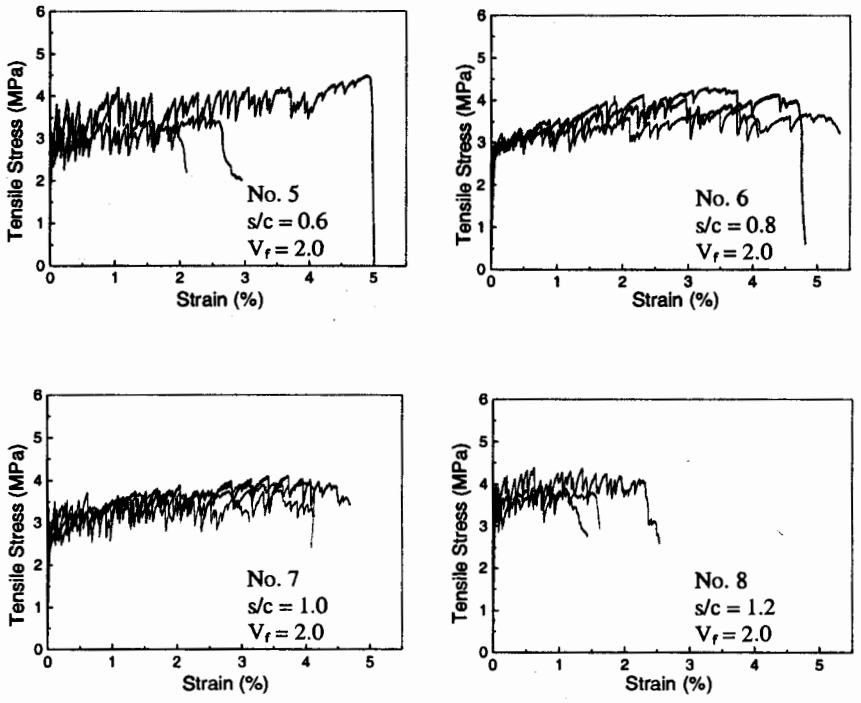

Fig. 6—Tensile stress versus strain curves of PVA-ECC (fiber with 0.5% oiling).

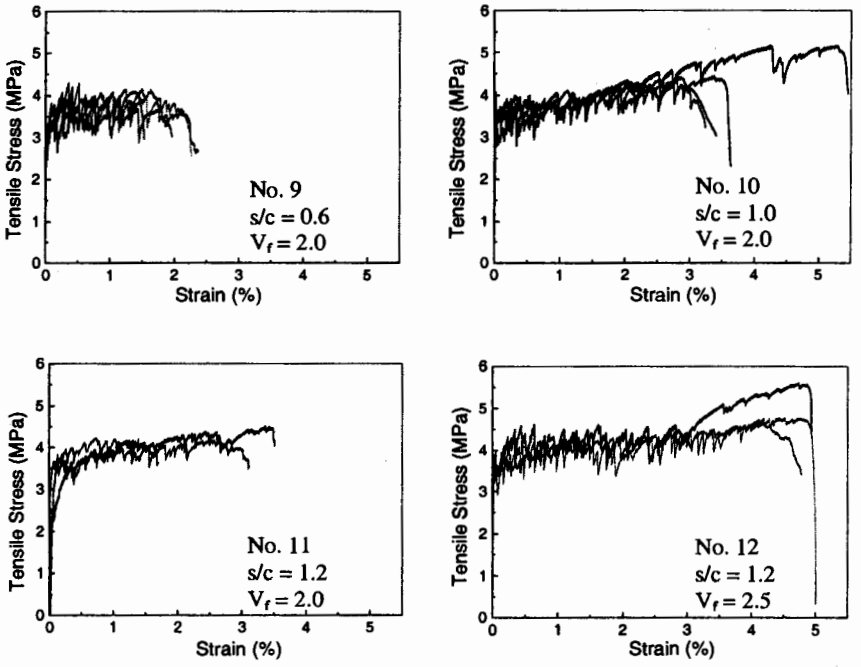

Fig. 7—Tensile stress versus strain curves of PVA-ECC (fiber with 0.8% oiling).

tion described by Eq. (1). The ultimate strength for this set of specimens is almost the same within the error range, while the mixture with $s/c = 0.6$ shows the best average strain capacity. The source of material property variation is likely due to different flaw size distribution and bridging property variation from specimen to specimen. The influence of flaw size distribution on strain-hardening has been discussed in Reference 31. The bridging property is likely to be negatively influenced by fiber breakage, and is discussed in the following section.

Significant improvement in ultimate strain is observed for the set of composites with 0.5% oiled fiber, and several specimens reach strain levels above 4%. The highest average strain of 4.18% is achieved at $s/c = 0.8$. Besides the increase in strain capacity, the property variation between specimens is clearly diminished. This improvement in performance consistency suggests a larger margin of satisfying the strain-hardening condition, and then in achieving fully saturated multiple cracking.[35] Compared with the composites with 0.3% oiled fiber, this set exhibits a small decline in first

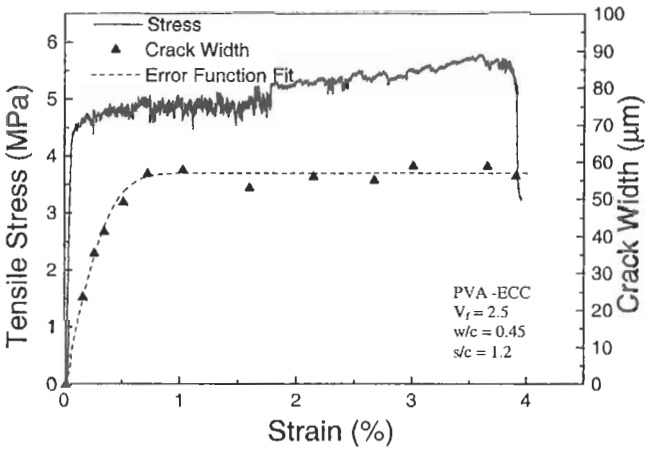

Fig. 8—Crack width versus strain relationship.

crack strength and ultimate strength. For the set of composites with 2.0% volume fraction of 0.8% oiled fiber, it appears that the mixture, at $s/c = 1.0$, outperforms the other two. One of the specimens achieves the highest ultimate strain of 5.2% at 5.0 MPa tensile stress. Mixture No. 12 has the same matrix as No. 11, but a higher fiber content of 2.5 vol %, which results in an increase of ultimate strain from less than 3 to nearly 5%. Moreover, Mixture No. 12 shows favorable performance robustness. Considering the cost constraint, however (the fiber is the biggest portion of the composite cost), low fiber volume fraction is preferred.

The ultimate strain ε_{cu} is determined by the number of multiple cracks developed and the opening of each crack. The crack opening listed in Table 3 was measured after unloading, which is approximately 70% of the opening at peak load due to the elastic recovery of the elongated fibers bridging across the matrix cracks. The actual average crack opening at peak load could be estimated from the ultimate strain (1.4 to 4.6%) and the average crack spacing (1.8 to 11.5 mm), giving a range of 80 to 160 μm. Because many microcracks that develop tend to completely close after unloading, which makes them very difficult to detect at the specimen surface, the average crack opening at peak load should be smaller than the aforementioned estimate.

Figure 8 shows a typical development of crack opening with an increase of strain. The monitored crack was one of several cracks that developed at an early stage of loading. Shortly after first cracking, the crack width grows rapidly with the increase of strain, and then stabilizes at approximately 60 μm while additional microcracks develop. This phenomenon was also observed on other ECC materials with intensive multiple cracking behaviors, whereas for typical FRC, the crack width almost linearly increases with load point displacement. For example, for the gage length used in this experiment (305 mm), the crack opening in a PVA-ECC 4% strain would approach 7.4 mm. For the PVA-ECCs investigated herein, it was found that the crack opening stabilization usually completes before 1% strain, and that the stabilized crack width ranges from 60 to 100 μm. Considering that water permeability scales with the third power of crack width[36] and that chloride permeability scales exponentially with crack width,[37] such small crack width in PVA-ECC implies significant improvement in durability of structures using PVA-ECC. To quantitatively describe the crack opening behavior,

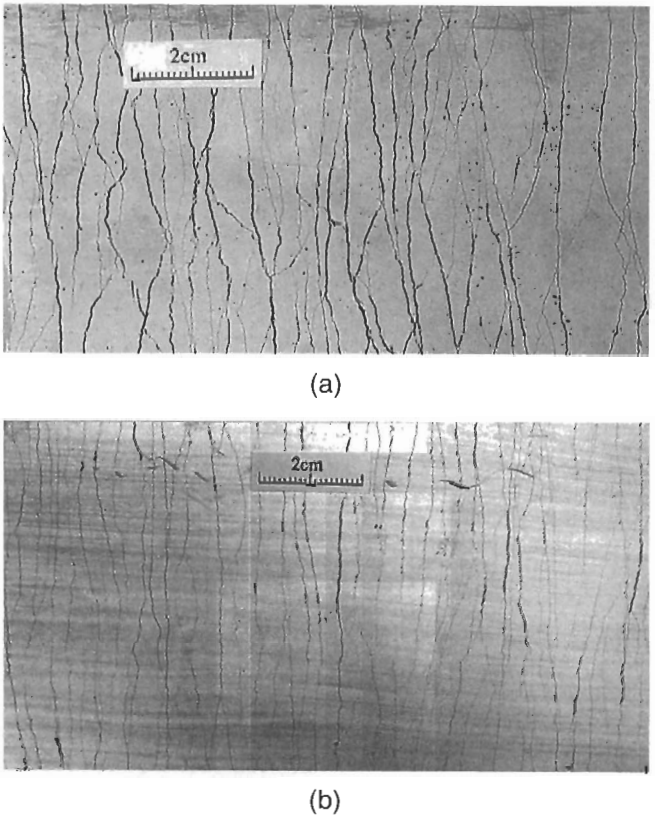

Fig. 9—Multiple cracking of PVA-ECC: (a) Specimen No. 10 (Fiber oiling agent 0.8%: V_f = 2.0%, s/c = 1.0); and (b) Specimen No. 12 (Fiber oiling agent 0.8%: V_f = 2.5%, s/c = 1.2).

the error function is chosen to fit the shape of the crack width δ versus strain ε relationship

$$\delta = A\ erf\ (B\varepsilon) \tag{4}$$

where

$$erf(x) = \frac{2}{\sqrt{\pi}}\int_0^x e^{-u^2}\,du \tag{5}$$

A and B are constants. As illustrated in Fig. 8, the agreement is satisfactory. For this particular case, A is 57 and B is 2.32. Figure 9 shows the saturated multiple cracking pattern of specimens No. 10 and 12. With a higher fiber volume fraction (2.5%), specimen No. 12 has smaller crack spacing than No. 10 (V_f = 2.0%).

DISCUSSION

PVA fiber features high interfacial frictional stress and strong chemical bond with the surrounding cementitious phases due to its hydrophilic nature, which can result in fiber surface damage during pullout process, as well as significant slip-hardening behavior.[38] Consequently, severe fiber rupture in composites was observed. Fiber surface oiling treatment can effectively alter the interfacial properties, especially the chemical bond G_d and frictional stress τ_0, which was verified by a single fiber pullout test.[33] For the 0.8% oiled fiber, the measured τ_0 and G_d approached the optimal values suggested by the micromechanics model between 1.0 and 1.7

Table 4—Interfacial properties and complementary energy J_b' for PVA-FRC and PVA-ECCs

Composite		PVA-FRC with RMU fiber	PVA-ECC with 0.3% oiled fiber	PVA-ECC with 0.5% oiled fiber	PVA-ECC with 0.8% oiled fiber
Interfacial properties	τ_0, MPa	3.6	3.5	2.5	2.0
	G_d, J/m^2	5.0	3.0	2.5	2.0
Complementary energy, J_b', J/m^2		0.5	9.6	10.7	16.5

MPa, and 2.0 J/m^2, respectively. In the context of the current matrix design and the achievable variation range of G_d and τ_{0r}, lower τ_0 and G_d leads to higher complementary energy, which leads to a larger margin for satisfying the pseudo strain-hardening condition and greater intensity in multiple crack saturation. For example, comparison between Mixtures No. 4, 7, and 10, which have the same matrix composition w/c = 0.45 and s/c = 1.0, clearly reveals the increasing trend of ultimate strain and decrease in crack spacing.

The presence of sand has two impacts on the micromechanics properties of composites, in terms of both matrix toughness and interfacial properties. A higher amount of aggregates is usually expected to increase the matrix toughness due to the increase of energy consumption by the tortuous crack-propagating path. The general trend of first crack strength for each set of tests, which shows a slight increase with the increase of sand content, supports this assertion under the assumption of similar maximum pre-existing flaw size in all composites. For the fine sand used in this research, however, which has a size (approximately 110 μm) approaching the size of cement grains (20 μm), its toughening effect was diminished. A high content of fine sand may also reduce the energy required to create a new fracture surface, as the binding energy between sand particles and cement should be lower than that between cement particles. Further investigation is needed to clarify this effect. High sand content may also cause higher interfacial frictional stress and, in turn, more severe fiber surface abrasion, resulting in deterioration in fiber bridging properties. In addition, recent research has reported that higher sand content could significantly increase matrix porosity when fiber is present.[39] This alteration of flaw size distribution also has an influence on pseudo strain-hardening behavior, as a large amount of pre-existing microflaws with a narrow size distribution is conducive to multiple cracking before peak bridging load is reached.[31] Observations in the present set of experiments seem to suggest that fiber with high oiling content also tolerates higher sand content, which leads to optimal performance when high oiling and sand contents are combined, as indicated by comparing Mixtures No. 2, 6, and 10. From the consideration of cost and shrinkage control, high sand content is preferable in practice, which validates the preference of a 0.8% oiled fiber instead of a 0.5% oiled fiber for structural applications.

To further highlight the effectiveness of the micromechanics-based tailoring procedure in PVA-ECC design, another PVA-FRC is introduced herein for comparison. The composite has the same mixture as No. 2 (w/c = 0.45, s/c = 0.6) and contains 2.0 vol % of PVA fiber trade-named RMU with fiber properties shown in Table 1. The fiber diameter is14 μm, and the length is 6 mm. In the context of PVA-FRC, where the fiber-matrix interfacial properties dominate the bridging behavior, a smaller diameter implies more severe

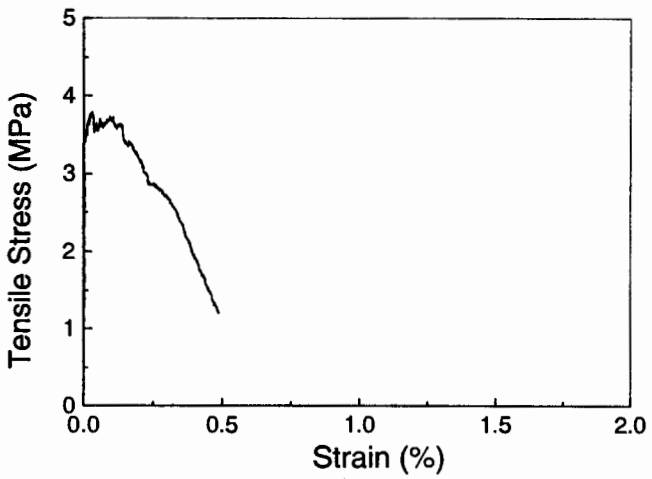

Fig. 10—Tensile stress versus strain curve of typical PVA-FRC. (RMU fiber: V_f = 2.0%.)

fiber rupture. The nominal strength of the RMU fiber is 1660 MPa, which is close to that of REC fiber, while the elastic modulus is 60 GPa, which is higher than that of RECREC fiber. No oiling agent was applied to the RMU fiber. Although the strengths of RMU and REC fibers are very similar, their composite performance is very different. The RMU-reinforced composite exhibits very marginal strain hardening behavior under uniaxial tensile loading (Fig. 10), with only several widely spaced cracks. At approximately 0.2%, the strain capacity is almost one order of magnitude lower than that of the PVA-ECC. The underlying reason for this difference in strain-hardening intensity lies in their significantly different complementary energies. Figure 11 shows the composite bridging stress versus crack opening relations for this PVA-FRC and for PVA-ECCs with three different oiled fibers, highlighting the clear distinction between PVA-FRC and PVA-ECC. The corresponding complementary energy is tabulated in Table 4. The interfacial properties based on single-fiber pullout tests[11,33] are also listed in this table. For the specific matrix of these composites, the crack tip toughness J_{tip} is approximately 3.2 to 4.7 J/m^2.[40] The steady-state cracking criteria (Eq. (1)) is therefore not satisfied by the PVA-FRC with RMU fiber (J_b' = 0.5 J/m^2), while the complementary energy of PVA-ECCs (J_b' = 9 to 17 J/m^2) are much larger than J_{tip}. This clearly explains why the PVA-ECCs exhibit ductile strain-hardening behavior, while the PVA-FRC shows quasibrittle tensile behavior. For the PVA-ECCs, different surface treatment results in the difference in complementary energy. When the oiling agent content of fiber increases from 0.3 to 0.8%, the corresponding complementary energy increases more than 140%, which gives a much larger margin for satisfying Eq. (1) for the development of strain-hardening.

As mentioned previously, PVA fiber tends to rupture during the pullout process. Higher chemical bond and frictional stress result in more severe fiber rupture and shorter fiber pullout length. The rapid drop of bridging stress of PVA-FRC in its $\sigma(\delta)$ curve (Fig. 11) reflects this trend. The scanning electron microscope pictures of fracture surfaces of the PVA-FRC and three optimal PVA-ECCs in each test set with different oiled fibers are presented in Fig. 12. The PVA-FRC, which contains a much larger number of fibers due to the small fiber diameter, shows a very short protruded fiber length (less than 0.2 mm) compared with that of PVA-ECC.

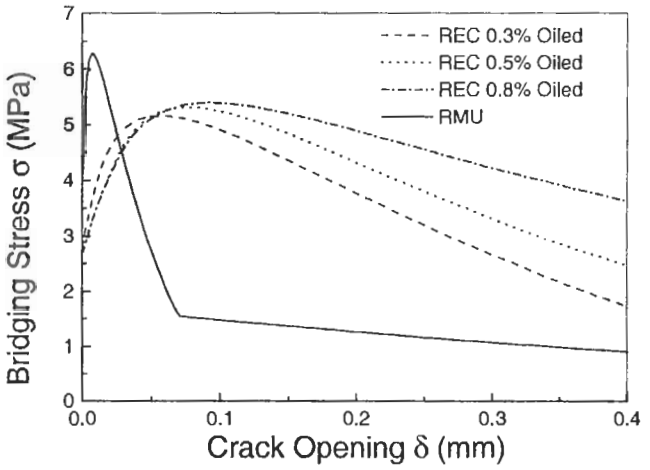

Fig. 11—Theoretical stress versus crack opening relationship of PVA-FRC and PVA-ECC. (V_f = 2.0%, w/c = 0.45, and s/c = 1.0.)

Inspection on the fiber ends indicates that most fibers in this RMU PVA-FRC were ruptured. The other three pictures clearly reveal the increasing trend of protruded fiber length with the increase of oiling agent content, reflecting the fact that oiling treatment can effectively reduce the bond and protect the fiber from premature rupture. The average protruded length for 0.8% oiled fiber (V_f = 2.0%) is nearly 2 mm, which is three times of that of the 0.3% oiled fiber. Fiber rupture was still observed in these PVA-ECCs; however, the extent was considerably alleviated, and the percentage of ruptured fiber diminished with the increase of oiling agent, as manifested by the increasing average protruded length. In these composites with crack spacing (Table 3) less than the fiber length, the protruded fiber length on the fracture surface is expected to be less than half the fiber length, even when all fibers are pulled out without rupture.

CONCLUSIONS

PVA-ECCs with satisfactory tensile behavior were developed under the PDDA. The guidance provided by the micromechanics models significantly speeds the composite design process. The uniaxial tensile tests conducted reveal robust pseudo strain-hardening behavior of PVA-ECCs. Ultimate strain exceeding 4%, as well as ultimate strength of 4.5 MPa, were achieved at a moderate fiber volume fraction of 2.0%. The specimens exhibited saturated multiple cracking with crack spacing of 2.5 and 1.8 mm for composites with V_f = 2.0 and 2.5%, respectively. It was also found that the crack opening soon stabilizes after rapid growth at the initial stage, reaching a steady state maximum crack width below 100 μm as the specimen strain increases in the multiple cracking process.

PVA fiber features high interfacial chemical bond, frictional stress, and slip-hardening in a cementitious matrix. The investigation on the effect of different fiber surface treatment on composite performance reveals the importance of interface tailoring. With a higher oiling agent content that lowers the chemical bond, interfacial friction, and surface abrasion (reported in Wu[33]), higher composite strain capacity and better performance consistency are obtained. Moreover, the optimal sand content increases with a higher oiling agent, at least in the range of sand and oiling agent content investigated in this study. Inspection of the fracture surface

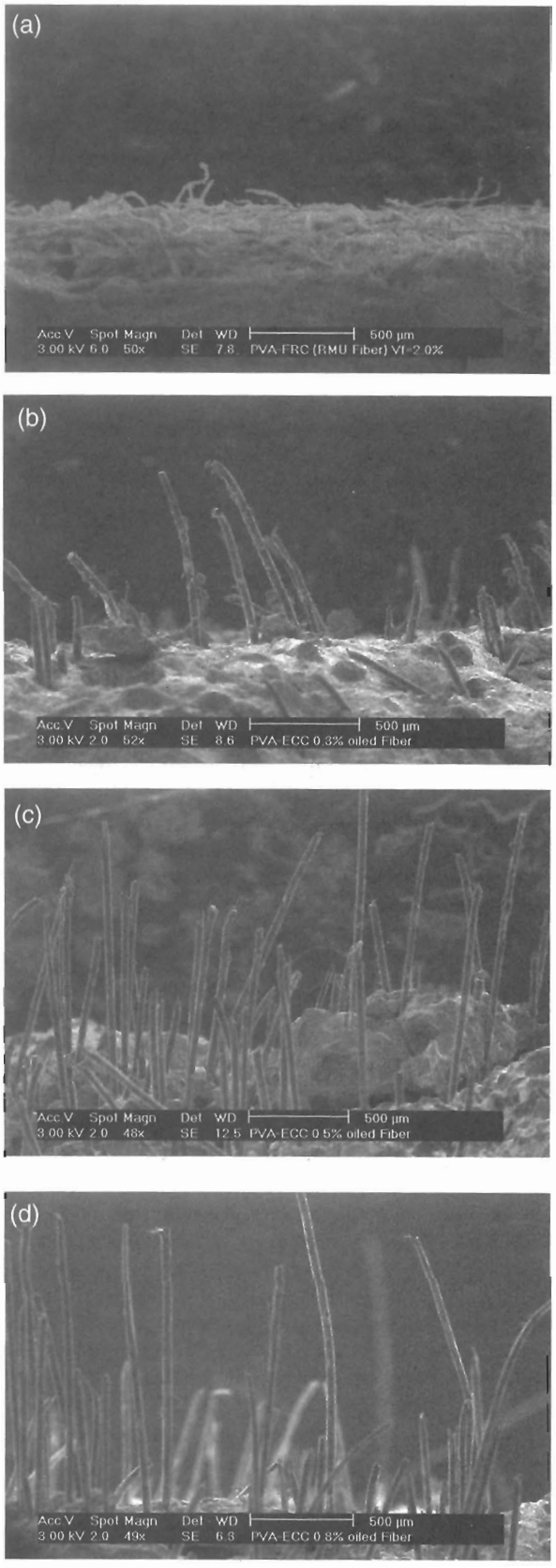

Fig 12—Protruded fibers at fracture surface: (a) PVA-FRC (RMU fiber V_f = 2.0%, w/c = 0.45, and s/c = 0.6); (b) PVA-ECC (0.3% oiled REC fiber: V_f = 2.0%, w/c = 0.45, and s/c = 0.6); (c) PVA-ECC (0.5% oiled REC fiber: V_f = 2.0%, w/c = 0.45, and s/c = 0.8); and (d) PVA-ECC (0.8% oiled REC fiber: V_f = 2.0%, w/c = 0.45, and s/c = 1.0)

shows increasing protruded fiber length with a decrease in interfacial bond properties, which is in accordance with the prediction of bridging stress-versus-crack opening relation.

The comparison of complementary energy between PVA-FRC and PVA-ECC highlights the underlying reason for their distinctly different tensile behavior. For PVA-FRC, the steady state cracking criteria are not satisfied, therefore it exhibits quasibrittle tensile behavior. For PVA-ECC, the complementary energy is much larger than the crack tip toughness, leaving sufficient margin to attain pseudo strain-hardening behavior. With lower interfacial bond properties corresponding to higher oiling agent content, the complementary energy is accordingly increased and results in more robust composite performance.

ACKNOWLEDGMENTS

Support by Kuraray Co., Ltd. (Osaka, Japan) is gratefully acknowledged. The authors would like to thank U.S. Silica Co. for providing fine sand. Valuable discussions with Gregor Fischer and Jun Zhang are acknowledged.

REFERENCES

1. Aveston, J.; Cooper, G. A.; and Kelly, A., "Single and Multiple Fracture," *Proceedings of Properties of Fiber Composites*, National Physical Laboratory, IPC Science and Technology Press, Guildford, UK, 1971, pp. 15-24.

2. Naaman, A. E., and Homrich, J. R., "Tensile Stress Strain Properties of SIFCON," *ACI Materials Journal*, V. 86, No. 3, May-June 1989, pp. 244-251.

3. Li, V. C., and Leung, C. K. Y., "Theory of Steady State and Multiple Cracking of Random Discontinuous Fiber-Reinforced Brittle Matrix Composites," *ASCE Journal of Engineering Mechanics*, V. 118, No. 11, 1992, pp. 2246-2264.

4. Li, V. C., and Wu, H. C., "Conditions for Pseudo Strain Hardening in Fiber Reinforced Brittle Matrix Composites," *Journal of Applied Mechanics Review*, V. 45, No. 8, 1992, pp. 390-398.

5. Naaman, A. E., "Tailored Properties for Structural Performance," *Proceedings of the RILEM/ACI Workshop: High-Performance Fiber-Reinforced Cement Composites*, E&FN Spon, London, UK, 1992, pp. 18-38.

6. Krstulovic, O. N., and Malak, S., "Tensile Behavior of Slurry Infiltrated Mat Concrete (SIMCON)," *ACI Materials Journal*, V. 94, No. 1, Jan.-Feb. 1997, pp. 39-46.

7. Breitenbucher, B., "High-Performance Fiber Concrete SIFCON for Repairing Environmental Structures," *Proceedings of the 3rd RILEM/ACI Workshop: High-Performance Fiber Reinforced Cement Composites*, H. W. Reinhardt and A. E. Naaman, eds., E&FN Spon, London, 1999, pp. 585-594.

8. Li, V. C., "Engineered Cementitious Composites—Tailored Composites through Micromechanical Modeling," *Fiber-Reinforced Concrete: Present and the Future*, N. Banthia, A. Bentur, and A. Mufri, eds., Canadian Society for Civil Engineering, Montreal, Canada, 1998, pp. 64-97.

9. Stang, H., and Li, V. C., "Extrusion of ECC Material," *Proceedings of the 3rd RILEM/ACI Workshop: High-Performance Fiber-Reinforced Cement Composites*, H. W. Reinhardt and A. E. Naaman, eds., E&FN Spon, London, 1999, pp. 203-212.

10. Li, V. C.; Fukuyama, H.; and Mikame, A., "Development of Ductile Engineered Cementitious Composite Elements for Seismic Structural Applications," *Proceedings of Structural Engineering World Congress (SEWC)*, Paper T177-5, San Francisco, July 1998.

11. Li, V. C., "Damage Tolerance of Engineered Cementitious Composites," *Advances in Fracture Research, Proceedings of the 9th ICF Conference on Fracture*, B. L. Karihaloo, Y. W. Mai, M. I. Ripley, and R. O. Ritchie, eds., Sydney, Australia, 1997, pp. 619-630.

12. Fukuyama, H.; Sato, Y.; Li, V. C.; Matsuzaki, Y.; and Mihashi, H., "Ductile Engineered Cementitious Composite Elements for Seismic Structural Applications," *CD Proceedings of the 12 WCEE*, 2000, Paper 1672.

13. Li, V. C., and Fischer, G., "Interaction between Steel Reinforcement and Engineered Cementitious Composites," *Proceedings of the 3rd RILEM/ACI Workshop: High-Performance Fiber Reinforced Cement Composites*, H. W. Reinhardt and A. E. Naaman, eds., E&FN Spon, London, 1999, pp. 361-370.

14. Fischer, G., and Li, V. C., "Structural Composites with ECC," *6th ASCCS International Conference: Steel-Concrete Composite Structures*, Y. Xiao and S. Mahin, eds., Los Angeles, Mar. 2000, pp. 1001-1008.

15. Li, V. C.; Mishra, D. K.; Naaman, A. E.; and Wight, J. K., "On the Shear Behavior of Engineered Cementitious Composites," *Journal of Advanced Cement-Based Materials*, V. 1, No. 3, 1994, pp. 142-149.

16. Kanda, T.; Watanabe, S.; and Li, V. C., "Application of Pseudo Strain-Hardening Cementitious Composites to Shear Resistant Structural Elements," *Fracture Mechanics of Concrete Structures Proceedings, FRAMCOS-3*, Freiburg, AEDIFICATIO04, Germany, 1998, pp. 1477-1490.

17. Maalej, M., and Li, V. C., "Introduction of Strain-Hardening Engineered Cementitious Composites in Design of Reinforced Concrete Flexural Members for Improved Durability," *ACI Structural Journal*, V. 92, No. 2, Mar.-Apr. 1995, pp. 167-176.

18. Li, V. C., and Hashida, T., "Engineering Ductile Fracture in Brittle Matrix Composites," *Journal of Materials Science Letters*, V. 12, No. 12, 1993, pp. 898-901.

19. Li, V. C.; Kong, H. J.; and Chan, Y. W., "Development of Self-Compacting Engineered Cementitious Composites," *Proceedings of International Workshop on Self-Compacting Concrete*, Kochi, Japan, 1998, pp. 46-59.

20. Shao, Y., and Shah, S. P., "Mechanical Properties of PVA Fiber Reinforced Cement Composites Fabricated by Extrusion Processing," *ACI Materials Journal*, V. 94, No. 6, Nov.-Dec. 1997, pp. 555-564.

21. Betterman, L. R.; Ouyang, C.; and Shah, S. P., "Fiber-Matrix Interaction in Microfiber Reinforced Mortar," *Journal of Advanced Cement-Based Materials*, V. 2, No. 1, 1995, pp. 53-61.

22. Shah, S. P.; Peled, A.; Aldea, C. M.; and Akkaya, Y., "Scope of High-Performance Fiber-Reinforced Cement Composites," *Proceedings of the 3rd RILEM/ACI Workshop: High-Performance Fiber Reinforced Cement Composites*, H. W. Reinhardt and A. E. Naaman, eds., E&FN Spon, London, 1999, pp. 113-129.

23. Cheyrezy, M.; Dugat, J.; Boivin, S.; Orange, G; and Frouin, L., "Concrete Comprising Organic Fibers Dispersed in a Cement Matrix, Concrete Cement Matrix and Premixes," *French Patent* PCT/FR99/01145, May, 1999.

24. Bentur, A., and Mindess, S., *Fiber-Reinforced Cementitious Composites*, Elsevier Applied Science, Essex, England, 1990.

25. Li, V. C., "From Micromechanics to Structural Engineering—The Design of Cementitious Composites for Civil Engineering Applications," *Journal of Structural Mechanics Earthquake Engineering*, JSCE, V. 10, No. 2, 1993, pp. 37-48.

26. Li, V. C.; Wang, Y.; and Backer, S., "Effect of Inclining Angle, Bundling, and Surface Treatment on Synthetic Fiber Pullout from a Cement Matrix," *Journal of Composites*, V. 21, No. 2, 1990, pp. 132-140.

27. Kanda, T., and Li, V. C., "Interface Property and Apparent Strength of High-Strength Hydrophilic Fiber in Cement Matrix," *Journal of Materials in Civil Engineering*, V. 10, No. 1, 1998, pp. 5-13.

28. Lin, Z., and Li, V. C., "Crack Bridging in Fiber Reinforced Cementitious Composites with Slip-Hardening Interfaces," *Journal of Mechanics and Physics of Solids*, V. 45, No. 5, 1997, pp. 763-787.

29. Marshall, D. B.; Cox, B. N., "A J-Integral Method for Calculating Steady-State Matrix Cracking Stresses in Composites," *Mechanics of Materials*, No. 8, 1988, pp. 127-133.

30. Lin, Z.; Kanda, T.; and Li, V. C., "On Interface Property Characterization and Performance of Fiber-Reinforced Cementitious Composites," *Journal of Concrete Science and Engineering*, RILEM, No. 1, 1999, pp. 173-184.

31. Wu, H. C., and Li, V. C., "Stochastic Process of Multiple Cracking in Discontinuous Random Fiber-Reinforced Brittle Matrix Composites," *International Journal of Damage Mechanics*, V. 4, No. 1, 1995, pp. 83-102.

32. Wang, Y.; Backer, S.; and Li, V. C., "A Statistical Tensile Model of Fiber Reinforced Cementitious Composites," *Journal of Composites*, V. 20, No. 3, 1990, pp. 265-274.

33. Wu, C., "Micromechanical Tailoring of PVA-ECC for Structural Applications," PhD thesis, University of Michigan, Ann Arbor, 2000.

34. Li, V. C.; Wu, H. C.; Maalej, M.; and Mishra, D. K., "Tensile Behavior of Cement-Based Composites with Random Distributed Steel Fibers," *Journal of the American Ceramics Society*, V. 79, No. 1, 1996, pp. 74-78.

35. Kanda, T., and Li, V. C., "Multiple Cracking Sequence and Saturation in Fiber Reinforced Cementitious Composites," *JCI Concrete Research and Technology*, V. 9, No. 2, 1998, pp. 19-33.

36. Tsukamoto, T., "Tightness of Fiber Concrete," *Darmstadt Concrete*, V. 5, 1990, pp. 215-225.

37. Wang, K.; Jansen, D.; Shah, S. P.; and Karr, A., "Permeability Study of Cracked Concrete," *Cement and Concrete Research*, V. 27, No. 3, 1997, pp. 381-393.

38. Redon, C.; Li, V. C.; Wu, C.; Hoshiro, H.; Saito, T.; and Ogawa, A., "Measuring and Modifying Interface Properties of PVA Fibers in ECC Matrix," *ASCE Journal of Materials in Civil Engineering*. (in press)

39. Akkaya, Y.; Peled, A.; Picka, J. D.; and Shah, S. P., "Effect of Sand Addition on Properties of Fiber-Reinforced Cement Composites," *ACI Materials Journal*, V. 97, No. 3, May-June 2000, pp. 393-400.

40. Li, V. C.; Mishra, D. K.; and Wu, H. C., "Matrix Design for Pseudo Strain-Hardening Fiber-Reinforced Cementitious Composites," *RILEM Journal of Materials and Structures*, V. 28, No. 183, 1995, pp. 586-595.